Indonesian Journal of Science & Technology

Heavy Oil Potentials in Central Sumatra Basin, Indonesia Using Remote Sensing, Gravity, and Petrophysics Data: From Literature Review to Interpretations and Analyses

Tri Muji Susantoro[1,2,], Suliantara[1], Herru Lastiadi Setiawan[1], Bambang Widarsono[3], Ketut Wikantika[4]*

[1]Research Centre for Remote Sensing, National Research and Innovation Agency, Jakarta, Indonesia
[2]Faculty of Earth Sciences and Technology, Institut Teknologi Bandung, Bandung, Indonesia
[3]Research Centre for Industrial, Process and Manufacture Technology, National Research and Innovation Agency, Jakarta, Indonesia
[4]Department of Geodesy and Geomatics, Institut Teknologi Bandung, Indonesia
* Corresponding author, email: trim010@brin.go.id

ABSTRACT

Central Sumatra basin is located on Sumatra Island, Indonesia, and is considered an oil prolific basin that produces heavy oil. The basin is believed to have unexplored heavy oil potential. Therefore, this study aims to map the heavy oil potential distribution in the basin using surface and subsurface lineaments analyses interpreted from satellite imagery and gravity data, and assisted by well log/petrophysics analysis. A thorough basin analysis was conducted based on surface/subsurface structures' control and source rock location settings to map all potential heavy oil traps. The gravity anomaly data interpretation identified the low areas and lineaments in NW – SE, and N – S directions. The interpretation of satellite imageries showed very similar lineament patterns with the same general direction. It was observed that there is continuity between subsurface and surface lineament features, which provide contact between reservoirs and surface water sources, thereby facilitating heavy oil generation. Overlapping the lineament interpretation of gravity and satellite imagery data, supported by petroleum system understanding and verification from wells data have confirmed 7 heavy oil trap potential areas within the sedimentary basin.

ARTICLE INFO

1. INTRODUCTION

Indonesia is facing critical challenges in energy policy management, regarding demands for energy security, climate protection, and a surge in energy demand. The continued export-oriented oil production aimed at meeting national revenue needs has led to a substantial decrease in oil reserves (Gunningham, 2013). Meanwhile, the ever-increasing domestic demand for energy, ultimately caused the country to be a net oil importer in 2006 (Pallone, 2009). The efforts made to discover new resources, include examining opportunities in heavy/extra-heavy oils and unconventional hydrocarbons. Therefore, this study focuses on heavy oil exploration in the Central Sumatra basin and broadly identifies the potential hydrocarbon resources in sedimentary basins on the island of Sumatra, Indonesia. In the Central Sumatra Basin, heavy oil's presence is indeed not something new. The large Duri field was discovered in 1941 with peak production of around 300,000 barrels of oil per day (BOPD) in 1994 (Sutadiwiria & Azwar, 2011; Winderasta *et al.*, 2018).

Heavy oil has a density of 10 – 22 in API gravity, which is approximately 934 to 1000 kg/m3 and usually with a viscosity larger than 100 centipoises (Gonçalves *et al.*, 2014; Guo *et al.*, 2016). According to Head *et al.* (2003), Meyer *et al.* (2007), and Meyer & Attanasi (2003), it occurs due to lighter oil's alterations through bacterial degradation, water washing, and evaporation. Furthermore, heavy oil is generally found at shallow depths with temperatures below 80 ºC (Head *et al.*, 2003; Hein, 2006; Meyer *et al.*, 2007), where there are contacts, such as faults and unconformities between reservoirs and the surface, groundwater aquifers, and/or shallow formation water. This condition often occurs at up-dip edges or flanks of large-scale foreland basins (Hein, 2006). However, oil biodegradation occurs at depths greater than 4 km, with most cases being at < 2.5 km (Head *et al.*, 2003).

This study aims to map heavy oil's potential distribution in the basin using surface and subsurface lineaments analyses interpreted with satellite imagery and gravity data, and supported by well log/petrophysics analysis. The lineament data are attributed to structural trends knowledge describing tectonic conditions, and are related to the presence of minerals, active faults, groundwater control, earthquakes, and geomorphology (Ahmadi & Pekkan, 2021; Epuh *et al.*, 2020). This lineament is expected to provide structural features acting as a fluid conduit to the subsurface, thereby establishing the potential for water washing and bacterial biodegradation on oil. The Landsat 8 Operational Land Imager (OLI) and Shuttle Radar Topography Mission (SRTM) data were used to map the surface geological features, while the gravity survey was used to map subsurface structures. After the correct geological environment for the heavy oil production has been found, well testing/sampling and laboratory fluid measurements are utilized to prove the heavy oil's presence. The approach adopted in this study is expected to contribute to the development of heavy oil in other sedimentary basins.

2. LITERATURE REVIEW

According to Leythaeuser (2005), hydrocarbons found in sedimentary basins are formed at a sufficient depth in the source rock layer, followed by a migration process, of which 75% is migrated, while 25% is left in the source rock. During the migration process, hydrocarbons are absorbed by minerals, leak to the surface, and are 40% trapped in the reservoir. The oil and gas trapped in reservoirs are reduced by chemical, physical, and bacterial processes over a long geological time, while only about 10% of it is explorable and producible.

The presence of oil and gas seepage on the earth's surface has been studied by Susantoro *et al*. (2020) on clay mineral anomalies in oil and gas fields. The seepage causes clay minerals to change into kaolinite, bleaching red beds, geobotany anomalies, and the presence of hydrocarbon-degrading bacteria (S. Chen *et al*., 2017; Petrovic *et al*., 2008; Schumacher, 1996). Ebulue (2022) discovered that the soil surface contaminated with oil and gas shows an increase in total petroleum hydrocarbons, increased activity of soil dehydrogenases, inhibition of soil catalase, and a decrease in pH over time. This condition also affects and stresses the surface vegetation (Susantoro *et al*., 2017). The hydrocarbon conversion to heavy oil occurs mostly in reservoirs that are lifted into the oxidation zone, resulting in water leaching, bacterial degradation, and evaporation (Meyer *et al*., 2007). Therefore, heavy oils are generally found at shallow depths associated with oil seeps, springs, tuff deposits, mud volcanoes, and close to faults or unconformities (Briggs *et al*., 1988; Head *et al*., 2003; Hein, 2017). According to Head *et al*. (2003), Hein (2017), and Meyer *et al*. (2007), shallow reservoirs with temperatures below 80 ºC are where anaerobic and/or aerobic bacteria that remove light hydrocarbons into heavy oil can survive. This is consistent with Rahayu *et al*. (2019) discovery that the biodegradation process is a site for hydrocarbon-degrading and phosphate-solubilizing bacteria's growth since crude oil consists of complex hydrocarbon compounds. Oil and gas biodegradation occurs when the reservoir is favorable for bacterial/microbial habitat. This is possible when: (1) the basement is lifted to a depth below 2 km for microbes to survive, (2) the basement is fractured for the permeability to be higher than the porosity of the matrix, (3) the oil-bearing provides a food source for microbes, (4) basement is high and the structure reacts to enable fluid movement and nutrient filling, and (5) the basement is lifted to the surface or near the surface and then reburied (Parnell *et al*., 2017). An example of this is found in the Llanos basin, where active uplift occurs, thereby resulting in a hydrodynamic flow associated with the oil-water contact and biodegraded oil due to bacterial activity (Macellari, 2021). Gregor (1997) found that the lineament structure is closely related to hydrocarbon migration and pooling from source to reservoir rocks, and an example is the Lloydminster area where hydrocarbons migrate to Mannville reservoirs. Similarly, oil fields in the Central Sumatra basin are mostly fault-controlled, in which oil migrates vertically from the Eocene-Oligocene Pematang Group Shale and laterally migrates eastward up the graben edge direction (Williams & Eubank, 1995).

Recent developments have shown intensive studies on nuclear magnetic resonance (NMR) logs, both at laboratory and field scales, to improve understanding of the interaction between NMR signals and heavy oil presence. Laboratory-scale studies have been performed to understand the relationship between NMR parameters, such as T_2 relaxation time and heavy oil-bearing rock's petrophysical properties at different thermal evolution (Li *et al*., 2022). Meanwhile, Zhou *et al*. (2021) examined the NMR and chromatographic characteristics of crude oil with different biodegradation levels. The result showed a set of maturity indices and biodegradation levels capable of helping heavy oil identification using NMR log data. Another recent study was also conducted by Markovic *et al*. (2020) on heavy oil NMR characteristics from 23 Canadian heavy oil reservoirs, which specifies the NMR viscosity model to be used when determining the oil viscosity being surveyed downhole. Consequently, heavy oils with typically high viscosity values were identified from the designed NMR log surveys.

Field studies were performed using NMR logs supported by other information sources, such as open-hole conventional logs, core, testing/sampling, and production data. For

example, Chakraborty *et al.* (2018) related the T_2 relaxation time and diffusivity contrast (D) of heavy oil when examining a heavy oil complex in Southern India. It was concluded that heavy oils are characterized by short T_2 and low D. Naik *et al.* (2018) performed a well-based study at the Greater Burgan field in Kuwait by combining NMR log data with its T_2 spectrum and production data from an electric submersible pump (ESP). The result showed specific characteristics for productive heavy oil zones in the field. Recently, Abd Al-Aali *et al.* (2022) identified tar-mat/bitumen using NMR log in the Zubair Formation, southern Iraq with the help of core and shallow resistivity log data. They were able to determine tar-mat/bitumen depth intervals in the field by examining T_2 shifting trends.

Despite NMR's effectiveness in identifying heavy oil's presence in sub-surface locations, its log data in oil fields is not always available. The efforts made by Chen *et al.* (2015) to overcome this deficiency were demonstrated through the utilization of a complete conventional open-hole logs data set and multi-mineral log interpretation assisted by permeability modeling, which identified heavy oil's presence from conventional open-hole logs. Heavy oil presence is therefore often identified using open-hole log data alone. Based on the literature review results above and **Table 1**, it is observed that the surface and subsurface lineament's interpretation is useful for identifying potential areas for heavy oil. The results are further verified with petrophysics data to increase the confidence level, thereby enhancing the detailed explanation of heavy oil's presence.

Table 1. Literature review as the basis for an integrated study of the potential for heavy oil in the Central Sumatra Basin.

Data	Methods	Study Area	Results	References
Oils Samples, Regional Geology	Lab. analyses (water high-pressure liquid chromatography (HPLC), Gas Chromatographic (GC), and GC-MS	Central Sumatra	API Gravity, Hydrocarbon profiles, bulk properties, Migration pathways facilitated by faults	(Hwang *et al.*, 2002)
ASTER DEM, Landsat 8 OIL/TIRS	Automatic lineament extraction, GPS for ground truth	Ugwueme, South Eastern Nigeria	Lineament is the migration path for hydrocarbon seepage	(Enoh & Okeke, 2021)
Surface lineaments & fractures, gravity & magnetic lineaments, Precambrian basement faults	Digitalizing, geological and mathematical analyses	Mid-Continent region	There is a consistency of surface lineaments with that of subsurface due to the fault system at the basement being reactivated many times and propagated upward to the surface. These acted for oil and gas trap development.	(Guo *et al.*, 1997)
Gravity and magnetic	Interpretation using Bouguer anomaly gravity and magnetization values of rocks	The Canterbury region	There is a consistency of subsurface structures resulting from gravity and magnetic interpretation with seismic data. The interpretation of gravity and magnetic anomaly data provided basic information for planning seismic surveys.	(Davy *et al.*, 2012)

Table 1 (Continue). Literature review as the basis for an integrated study of the potential for heavy oil in the Central Sumatra Basin.

Data	Methods	Study Area	Results	References
Gravity and magnetic	Interpretation using Bouguer anomaly gravity and magnetization values of rocks	The Canterbury region	There is a consistency of subsurface structures resulting from gravity and magnetic interpretation with seismic data. The interpretation of gravity and magnetic anomaly data provided basic information for planning seismic surveys.	(Davy *et al.*, 2012)
Remote Sensing data, geological, geophysical, geochemical, and hydrological maps	Correlations among data to identify petroleum and potash mine extensions	Saskatchewan and Alberta	Long lineaments correlated with Precambrian basement, surface, and subsurface lineament concentrations associated with repeated geological activities including subsidence and uplift, hence they are useful for determining oil and gas deposits.	(Penner & Mollard, 1991)
Gravity	Anomaly interpretation using Gravity and Magnetic Interpretation (GMINTERP).	Biga and Gelibolu peninsulas	General anomaly patterns of the subsurface corresponded to surface geology	(Ekinci & Yiğitbaş, 2015)
Field samples of heavy oil seepages	Bacteria biodegrading heavy oil identification and GIS analyses	Central Sumatra	Distribution of probable lower limit of heavy oil-bearing zones	(Hadimuljono & Firdaus, 2021)
SAR and Gravity	Edge techniques using automatic computing, and Bouguer gravity anomaly	Mahanadi basin, Eastern India	Tectonic features in the surface well correlate with the gravity gradient trends and also gravity lineaments well correlate with faults in the shallow crust.	(Satyakumar *et al.*, 2022)
Gravity	Spectral analysis, the Gaussian filter, and the first horizontal derivative	Lamu Basin, South Eastern Kenya	Map of anticline and syncline structures, thick sedimentary successions in basement high and low to represent good hydrocarbon source kitchens.	(Ombati *et al.*, 2022)
Open hole log data of well data and fluid sampling/lab test data	Standard open-hole log interpretation to identify oil-bearing intervals. Confirmation of heavy oil presence is assisted by well-test/sampling data.	General	Evidence of heavy oil presence in wells that are used for verification over indication given by lineament.	(Darling, 2005)
Landsat 8 OLI, SRTM DEM, Gravity Data, and Petrophysics data	Manual and automatic interpretation, ground surveys, correlation, petrophysical analyses	Central Sumatra	Heavy oil potential areas	This work

3. METHOD

3.1. Geology of Central Sumatra Basin

The Central Sumatra Basin (CSB) developed during the late cretaceous to early tertiary as a result of the India-Australia plate, which subducted the Southeast Asia plate to form a back-arc setting (Hwang *et al.*, 2002). Tectonically, this basin has two dominant fault directions, namely a northward fault paralleling the Malaysian structure and a younger one towards the northwest parallel to the Semangko fault, which is characterized by the presence of

horst, graben structures, and trans-current faulting (Mertosono & Nayoan, 1974).

The CSB is associated with the petroleum lacustrine system formed at the same syn-rift stage with the Pematang – Pematang petroleum system – fluvial and alluvial fan reservoirs, as well as Pematang – Duri petroleum system - fluvio-marine and carbonate platform reservoirs. In addition, the basin has a main reservoir in the pre-rift (basement) or younger stages with Duri Formation as a fluvio marine and carbonate platform in inversion anticlines and drape structures, which were formed in the second syn-rift phase. It further has reservoirs in Sihapas Formation with fluvial, fluvio-marine, and marine reservoirs inversion anticlines as well as stratigraphic traps in the Late Syn-rift (Doust, 2017). The CSB was proven to have heavy oil fields, such as the giant Duri field and Batang, located northwest of the Duri field. The analysis of 44 oil samples from 31 production fields in the CSB's North Aman, South Balam, and Rangau Troughs showed that six fields produced heavy oil (Hwang *et al.*, 2002). Geographically, the CSB is located in and around Riau province on Sumatra Island, Indonesia as shown in **Figure 1**.

3.2. Data Processing

The surface data sets utilized are Landsat 8 OLI path/row 126/059, 126/060, 127/059, and 127/060, and SRTM downloaded from https://earthexplorer.usgs.gov. This data was used to map the geological structure surface, known as lineament. The needed gravity data for subsurface lineament were downloaded from https://topex.ucsd.edu and used to map subsurface geological structures in the CSB.

The well log and testing/sampling data for petrophysics analysis were obtained from the Special Task Force for Upstream Oil and Natural Gas Business Activities (SKK Migas) at the Ministry of Energy and Mineral Resources (MEMR) as well as the Centre of Data and Information (Pusdatin) at the MEMR. Supporting data in the form of laboratory analysis results were acquired from the Research and Development Centre for Oil and Gas technology called "LEMIGAS" MEMR.

A field survey was performed to collect heavy oil seep/spill sets in the CSB, which were later sent for laboratory analysis to measure their API gravity and identify the predominant heavy oil biodegradation bacteria.
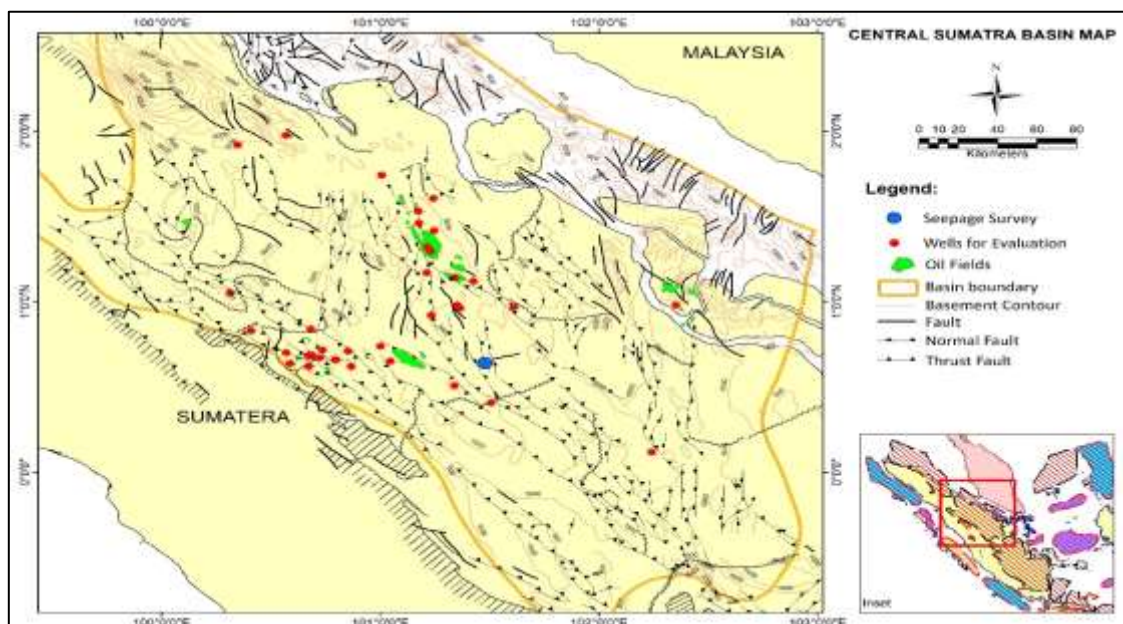

Figure 1. The Central Sumatra Basin on Sumatra Island, Indonesia, overlaid with a basement structure (source: Beicip-Pertamina, 1985; BPMIGAS-LAPI ITB, 2008).

Landsat 8 OLI data processing consists of (1) radiometric correction using The Fast Line-of-sight Atmospheric Analysis of Spectral Hypercubes (FLAASH) method, (2) mosaic 4 Scenes Landsat 8 OLI, (3) composite 567 (RGB), and (4) the combination of the composite image with SRTM to facilitate interpretation on lineaments. Structural presence in satellite imageries was indicated by 1) river flow or straight valleys, 2) regular river bends inducible as straight lines, 3) the relationship between the main river and its tributaries, which are perpendicular to each other, 4) shifting rock formation layers, 5) straightness of triangle-facets rows, and 6) extreme lithology offsets or topographical changes. It is important to note that this appearance is commonly referred to as lineament and it is interpreted based on automatic extraction using SRTM DEM data processed into a shaded relief image lightened with multiple illumination directions at 0, 45, 90, and 135° azimuths. Multiple methods are used in lineament interpretation because they produced accurate distribution, unlike the single (Ahmadi & Pekkan, 2021).

In addition, the subsurface lineament's interpretation was performed on the free air anomaly gravity (FAA) map of the study area, which was manually supported by an understanding of regional geological conditions. According to Sandwell *et al.* (2014), the gravity anomaly data utilized was measured through a pair of satellites flying in the same orbit, with an accuracy close to 1.4 mgal. Davy *et al.* (2012) discovered that the data provided subsurface information and has a good correlation with seismic interpretation. It showed dense, shallow igneous intrusions, and anomalously dense lower crust. It was observed that the gravitational field strength value in sedimentary rocks was generally smaller compared to the igneous. This simply implies that when the sedimentary rock becomes thicker, the gravitational field value reduces. Therefore, the gravitational field strength

map was useful for identifying low and high areas. The rate of change in the field strength value was useful in detecting subsurface fault structures. The gravity interpretation in this current study focused on high and low areas analyses, as well as faults developed in the basement rock (Hildenbrand *et al.*, 2001).

3.3. Field Survey and Laboratory Analyses

Heavy oil samples were obtained through a field survey and were later analyzed to determine their specific gravity in °API, as well as the bacteria type causing the oil biodegradation. The identification of oil biodegradation bacteria was performed to prove that an important factor in heavy oil formation at CSB was caused by bacteria. **Figure 1** shows the sampling location, represented by a blue dot. The oil's specific gravity analysis was conducted at the Distillation Laboratory – "LEMIGAS", while the bacteria were identified at the Research Centre for Biology, namely National Research Institute (LIPI) using the PCR method with document number FR-CC.03-02. The heavy oils obtained from the field sampling were tested with three bacterial isolates. Meanwhile, other data such as oil density were collected from previous laboratory analysis results (i.e., LEMIGAS database) and various literature, specifically the Indonesian Petroleum Association (IPA).

3.4. Analyses of Heavy Oil Distribution

The analysis to identify heavy oil distribution based on surface integration and subsurface data was conducted through the following stages:

(1) Interpret the surface and subsurface lineament based on Landsat 8 OLI and SRTM DEM, as well as gravity data, respectively. The Landsat 8 OLI lineament data were interpreted manually and automatically into four viewpoints, namely 0°, 45°, 90°, and 135° azimuths to respectively produce five types of surface lineament and process diagrams. Meanwhile, the gravity lineament

data were only interpreted manually to produce subsurface structures.

(2) Overlay the surface and subsurface lineament interpretation results to identify their continuity and assess the existing heavy oil field characteristics.

(3) Perform an initial analysis of heavy oil's presence in the Duri field based on the results of the surface and subsurface lineament overlays as a reference for mapping its distribution in the CSB. The analytical results were the geological characteristics of the existing heavy oil location.

(4) Identify the potential for heavy oil throughout the CSB based on references established in the previous stage, specifically point 3. The analysis conducted at this stage is to identify the characteristics of the areas that are following the existing heavy oil locations to pinpoint and map their distribution.

(5) Prove the heavy oil locations using petrophysics analysis on well log data as well as data from laboratory analysis and other references.

The detailed confirmation of heavy oil distribution based on petrophysical analysis of well log data was conducted at several key locations. Specifically, the petrophysics analysis was performed with a qualitative log to identify shallow oil-bearing permeable zones by interpreting the standard open hole logs of gamma-ray/spontaneous logs, resistivity, which is mostly induction, the porosity of neutron, density, and acoustic logs.

Quantitative analysis was added to get ideas of rough petrophysical properties, such as porosity and oil saturation by using standard quantitative methods in open-hole log analysis (Asquith and Krygowski, 2004). Information from laboratory fluid analysis and other sources or references were later used for confirmation. (6) Map the distribution of heavy oil potentials throughout the Central Sumatra basin.

4. RESULTS AND DISCUSSION
4.1. Surface Lineament

The surface lineament interpretations performed manually and automatically showed relatively the same general directions of N - S and NW - SE except for the 135° azimuth, which indicated a preferential NE - SW direction. The dominant N - S lineament direction was considered an old structure parallel to Malaysia's structural trend, while the NW - SE direction was a younger lineament parallel to the Semangko fault (Mertosono & Nayoan, 1974). In manual interpretation, the resulting lineament is not as much as those extracted automatically. However, the manual interpretation has considered the regional tectonic force's existence at the study site based on local geological knowledge from the interpreter's perspective. **Figure 2** shows that the total manual lineament was 646 lines with a total length of 5,722 km.

Based on the manual interpretation of the lineament, a detailed analysis was performed at 7 areas, labeled 0 to 6 in order to identify the lineament's direction as shown in **Figure 2**. It was observed that there is no significant difference in the lineament's direction between each of the areas. In other words, the predominant lineament's direction is generally similar, namely the N-S/NW-SE. However, it is still possible to identify the recent surface lineament in the E-W direction at areas 1, 3, 4, 5, and 6. **Figure 2** shows that the NE-SW direction is also found in areas 1, 4, and 6. As previously described, detailed auto lineament was divided into four viewing angles or azimuth at 0, 45, 90, and 135°, with each having different total lines and lengths as seen in **Figure 3**.

In **Figure 3a**, the auto lineament at 0° azimuth has 5,201 lines with a total length of 28,475 km in NW-SE, W-E, and E-W directions. At 45° azimuth, it has 5,249 lines with a total length of 29,490 km in the N-S direction as shown in **Figure 3b**. According to **Figure 3c** the auto lineament at 90° azimuth has 5,944 lines with a total length of 31,938

km in NW-SE, NW-SE, and NE-SW directions, while in **Figure 3d,** the lines were 9,297 at 135° azimuth with 48,454 km length in the NE-SW direction. The rose diagram results of all auto lineaments combined at 0, 45, 90, and 135° azimuths were shown in **Figure 3e**.
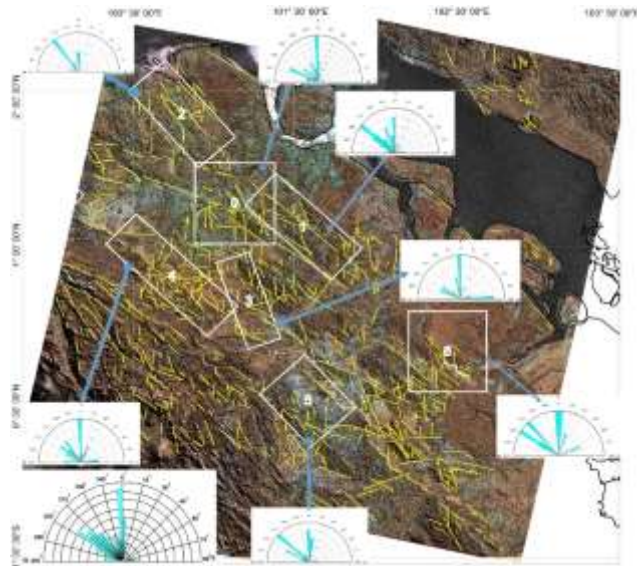

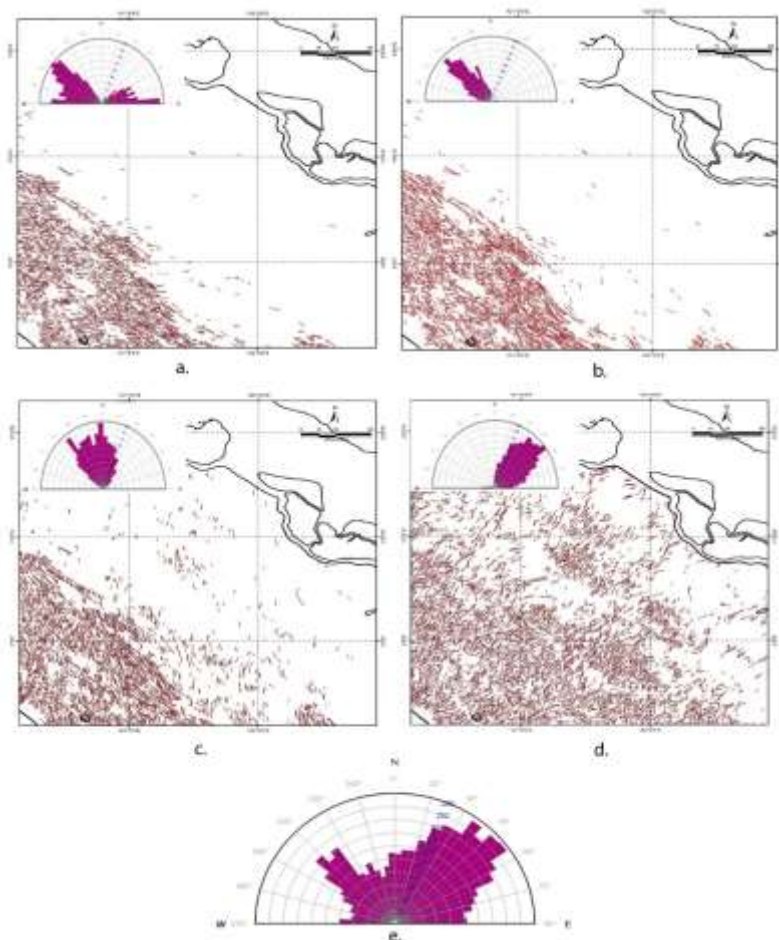**Figure 2.** Manual lineaments interpreted from Landsat 8 OLI combined with SRTM DEM.

Figure 3. Automatic lineaments: (a) Azimuth 0°; (b) Azimuth 45°; (c) Azimuth 90°; (d) Azimuth 135°; and (e) Combined lineaments rise of 0°, 45°, 90°, and 135°.

It was observed that the auto lineament at 0° azimuth still reflects a younger fault trend in the NW-SE direction, while the W-E direction is likely to be recent and/or only vegetation, cultural, and other lineaments. Auto lineament at 45° azimuth is predominantly in the NW-SE direction, indicating a young fault parallel to the Semangko fault. At 90° azimuth, the auto lineament has the same direction as the manual, namely in N-S and NW-SE, hence it was denoted as old and young faults reflection in the Central Sumatra Basin.

According to **Figure 3d,** the lineament pattern produced at 135° azimuth was different from others, namely NE-SW. Therefore, it was considered a recent joint, which partly mixed with the vegetation morphology and other cultivated objects' appearance generally in the NE-SW direction. This condition was not following the general geological structure developed in Sumatra, which lies in NW-SE and N-S directions. It was found that the most corresponding result to the manual interpretation was 90° azimuth. These facts explained that the automatic lineament identification was unable to distinguish pure geological process results from human engineering or man-made processes and recognize lineament's existence parallel to the azimuth's position.

The lineament structures in the southwest part of the study area were generally identified manually and automatically. This area has a high morphological contrast, based on ground truth revealing rock formations of the Pre-Tertiary age, Pematang, Sihapas, Telisa, and Petani. Meanwhile, it is impossible to automatically detect the lineament's presence in the eastern part because the location has morphological conditions with low contrast. At this location, several relatively young rock formations were exposed, including the Petani, Minas, and Alluvial Deposits (Suwarna *et al.,* 1994). Regarding lineament interpretation, there are generally major and minor structures spread over old to young

rocks (Pre-Tertiary – Quarter) in the study area. It was estimated from the existing major/dominant lineaments that the tectonic phase at work was at the Late Cretaceous age, while the minor trend was at the Early Miocene and Plio-Pleistocene tectonic ages.

This is consistent with Mertosono & Nayoan (1974) that a Late Cretaceous tectonic phase existence caused fault formations in the N-S and NW-SE directions. This formed the horst-graben series, trending the N-S and controlling the sedimentation in Lower Tertiary. It was observed that this major structure experiences movement again in younger tectonic, being the Early Miocene and Plio-Pleistocene with evidence of the same lineament pattern in rock formations aged Plio-Pleistocene.

Based on the manual analysis results of lineament density, oil and gas fields were distributed from low to high categories as shown in **Figure 4.** However, for heavy oil fields at the edge of the lineament density, the category is high to medium. Guo & George (1999) described the surface lineament that is consistent with gravity orientation and subsurface faults as the locus for oil and gas traps, while Boucher's analysis shows there is a relationship between lineament and the occurrence of oil and gas formation (Boucher, 1995).

Lineament's existence provides fairways for turbidite flow as well as pathways for salt emplacement and hydrocarbon migration (Gao & Milliken, 2012). It is further suspected that the continuous surface lineament to the subsurface is possibly one of the causes of oil biodegradation. This is because, when the oil had accumulated in the reservoir, surface water flows into the subsurface through the lineament to occupy the oil-filled reservoir. This cooled down the reservoir, thereby allowing the microbes to flourish and degrade the oil into heavy oil.

It was observed from **Figure 4** that the lineament density results from auto analyses at 0°, 45°, and 90° azimuths differ from those

produced manually. In the auto lineament, high density was found only in the part of the Sumatra fault zone located at the south of the CSB. Meanwhile, almost all the oil and gas fields exhibited low density. For example, at 135° azimuth, oil and gas fields were distributed at a very low to high density, while the heavy oil fields were distributed at a very low to low density. The difference between lineament density mapping results of manual and automatic interpretation was that the manual was always supported by knowledge of regional geology and selective geographical areas of interest. For example, the southwest side is not an area of interest because reservoir and cap rocks in the area have been exposed and even eroded, hence no interpretation was conducted. Meanwhile, the auto lineament identification only considers morphological contrast aspects, topographic differences, and variations in vegetation patterns and culture. This means when the difference is low, it is impossible to identify the lineament's structure. Another shortcoming of this method was its inability to identify structures aligned with the azimuth point of view, which means in relatively flat areas having low morphological contrasts, it is unable to identify the structural presence.
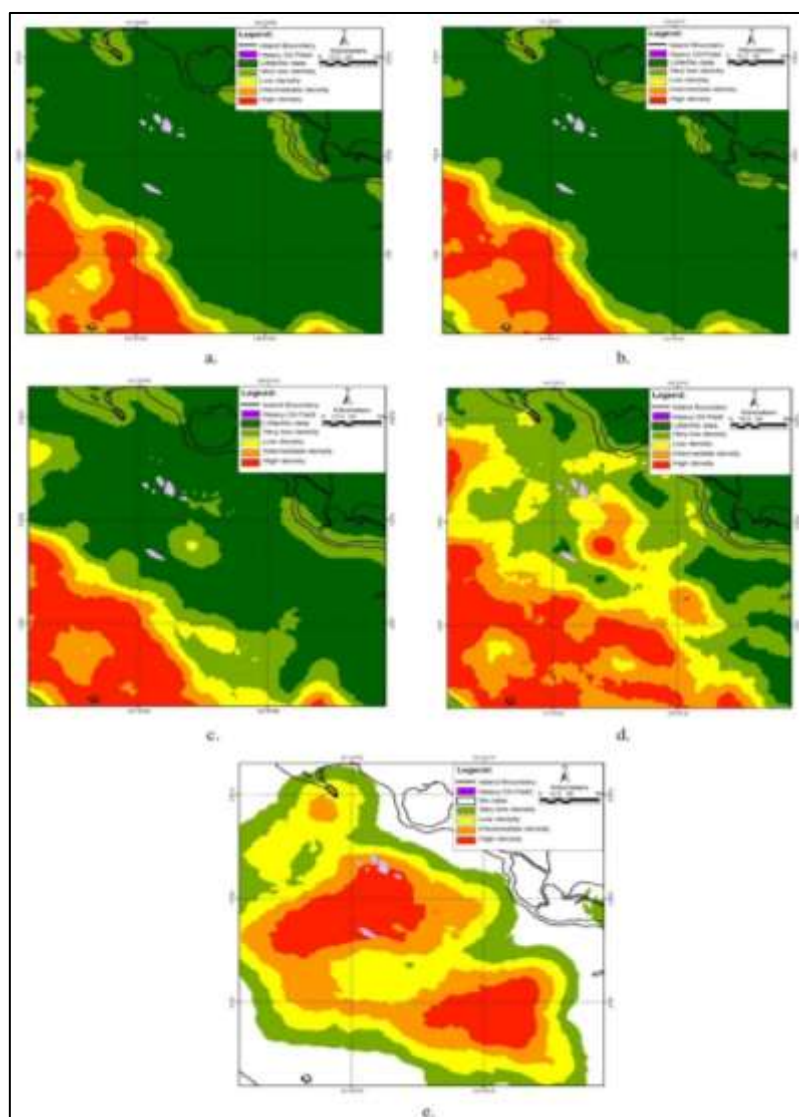

Figure 4. Lineament density resulted from automatic lineament interpretation: (a) Azimuth 0°, (b) Azimuth 45°, (c) Azimuth 90°, and (d) Azimuth 135°, and (e) result of manual interpretation.

4.2. Subsurface Lineament

Based on **Figure 5,** the free air anomaly (FAA) gravity survey data at the study site were between -231 mgal to +187 mgal. In the southwest, which is parallel to the west coast of Sumatra, the FAA values tend to be high positive (28 – 168 mgal) in the NW–SE direction. At the northeastern part parallel to the east coast of Sumatra, the FAA value was relatively uniform and high positive (28-48 mgal) in the NW-SE direction. This pattern was in line with the Sumatran fault system, which is a dextral due to collision from the Eurasian and Indo-Australian Plates movement to the south and north, respectively (Agustin *et al.*, 2019; Setiadi *et al.*, 2021). The FAA value was used in estimating the rock basement position. When the value is high, the basement position is suspected to be on the surface or close to the earth's surface while, when it is low or even negative, the bedrock is assumed to be far from the earth's surface and the area consists of very thick sedimentary rocks.

The lineament interpretation results on the FAA map show the general direction of N–S and NW–SE, which is similar to the surface lineament structure. According to Doust (2017), the structural direction was considered to have experienced movement in the Late Cretaceous tectonic and controlled the sedimentation process in the Lower Tertiary. It is therefore interpreted from the subsurface structure that the estimated lineaments separated the low and high areas. The structure was also observed to serve as a facility for oil and gas migration from the source rock to the reservoir. Based on the plot, the lineament direction in the rose diagram shows that the main directions were N315°E and N0°E as shown in **Figure 5**. These results showed that gravity was useful for detecting geological features, such as major and minor faults (Aydogan, 2011; Darmawan *et al.*, 2021).

The subsurface lineament results showed the same direction/orientation pattern as the dominant surface lineaments in the N-S and NW-SE directions. This indicates several subsurface fault reactivations were repeated and extended to the surface. This is consistent with Guo *et al.* (1997) discovery that the consistency of surface and subsurface lineament orientation occurred due to repeated reactivation of the subsurface fault system, causing it to spread to the surface. Also, Boucher (1995) confirmed that lineament was a surface expression of deeper features, such as subsurface.
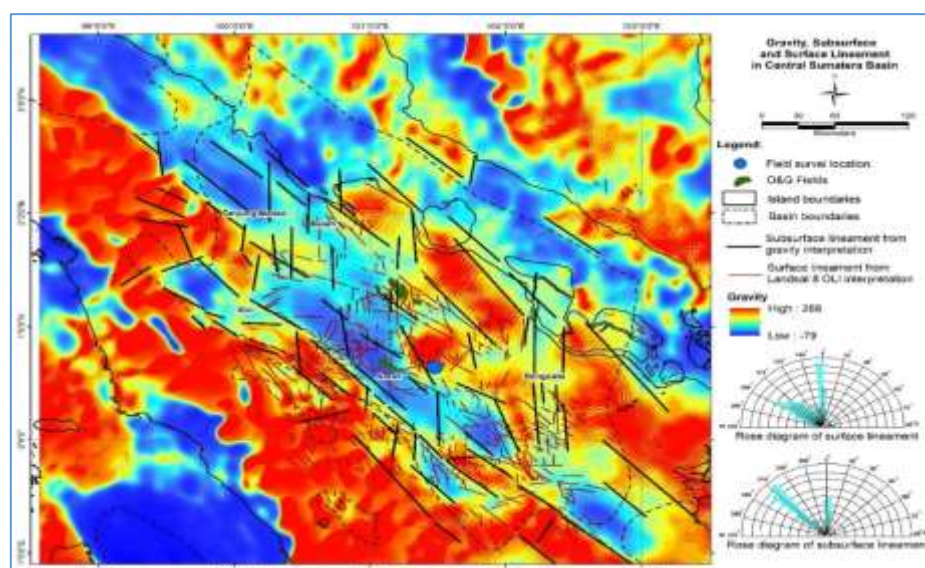

Figure 5. FAA values and the lineaments interpretation. Proven (i.e producing) heavy oil fields (in green) are situated on the horst edge, facing to graben.

4.3. Analyses of heavy oil distribution

Based on the FAA analysis of existing heavy oil fields, namely Duri, Batang, Kulin, and Rantaubais where low values described the source rock locations, results showed that heavy oil in CSB was formed on the edge of the horst facing the graben. This is well depicted in section AA', showing that the existing heavy oil field, e.g Duri was at the horst's edge as seen in **Figure 6a**.

This heavy oil field is located in a medium FAA value area, while the one above is located between low and high FAA values to the west and east, respectively. According to Widarsono *et al*. (2021), oil fields producing heavy oil are at depths of 150 – 700 m, but there are heavy oils at 50 – 300 m and 700 – 1,565 m depths that were yet to be produced. The existing heavy oil field location was found at subsurface lineaments with N–S and NW–SE directions intersecting each other. In **Figure 5**, these subsurface lineaments separate the heavy oil field from the graben. Further analysis showed the lineament as the oil migration path from the kitchen located in the graben area, namely the Aman Trough. As explained by Rodriguez and Philip, the main source rock is Paleogene from the Pematang Brown Shale Formation in Aman Trough. However, oil-producing areas also include Balam, Kiri, Tanjung Medan, and Bengkalis troughs (Rodriguez & Philip, 2012; Rodriguez & Philip, 2015).

As earlier mentioned, the existing heavy oil field location of the subsurface lineament shows the same pattern as the surface with N–S and NW–SE intersecting each other. However, the auto lineament results of the surface at 0° and 45° azimuths did not show any straightness, except for 90° azimuth in the NNW-SSE and NNE-SSW directions. The auto lineament at 135° azimuth appears to be quite tight with the relatively dominant NE-SW direction. In **Figure 4d**, the analysis shows that the density lineament at 135° azimuth relatively reflects subsurface conditions, with horst being sufficiently indicated by high density. A cross-sectional analysis was performed on lines AA', BB', CC', and DD' to identify heavy oil's presence representing CSB conditions as shown in **Figure 6**. This is based on a consideration that the section crossing high and low FAA values in Aman, Bengkalis, Balam, Kiri, and Tanjung Medan troughs areas are sub-basins of source rocks in the CSB. Another consideration is that the cross-section passing through lineaments is the intersection zone in the N–S and NW–SE directions, both in the subsurface and on the surface.
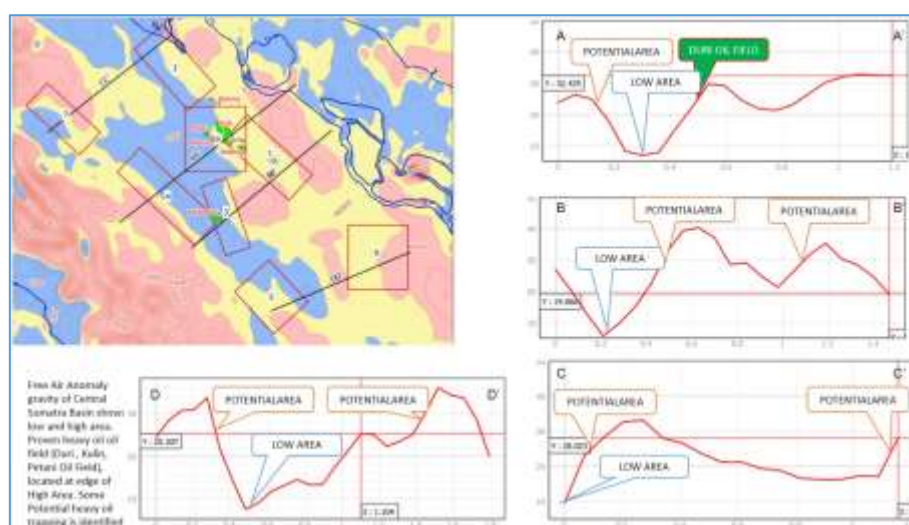

Figure 6. High – Low area map, proven/existing hydrocarbon fields, potential areas, and cross sections of FAA values.

The results show that areas identical to the existing heavy oil fields potentially contain heavy oil, denoted as red squares in **Figure 6**. It was observed that the continuous lineament on the surface supported water entry into the earth or reservoir and is considered a factor for the biodegradation of lighter oils into heavy oil. Head *et al.* (2003); Meyer *et al.* (2007); Meyer & Attanasi (2003) gave an opinion that heavy oil occurred from light oil alteration, especially due to water washing. As shown in **Figure 6**, Potential Area 1 is found 45 km southeast of the existing heavy oil fields, with a medium FAA value and lineaments in the N315°E direction. Potential Area 2 is located 70 km northwest of the existing heavy oil fields with a medium FAA value as well as lineaments in N315°E and N0°E directions.

The oil in Potential areas 1 and 2 generally came from the Aman and Balam troughs, migrating to the east and north. Furthermore, Potential area 3 is located 70 km south of the Duri areas, with a medium FAA value and several lineaments in the N320°E direction, hence the oil is predicted to fill the area through a vertical migration process from the Aman Trough. Potential area 4 is situated 60 km southwest of the Duri area with a medium FAA value and is expected to receive hydrocarbons, which migrate westward from the Aman Trough. Potential area 5 is situated 150 km to the south of the Duri area, with an intermediate FAA value and lineaments in N315°E and N0°E directions. The area is estimated to receive hydrocarbon filling migrating vertically and in the south from the Aman Trough. Potential Area 6 is located south of Bengkalis Trough with medium FAA value and lineaments in N0°E direction and is predicted to receive hydrocarbons that migrate eastward. Potential Area 7 with a medium FAA value, is characterized by lineaments in N340°E and 320°E directions and is expected to receive hydrocarbon filling migrating vertically and to the northwest from the Kiri Trough.

4.4. Verification of Heavy Oil Distribution

Heavy oil's presence was verified on oil seepage samples obtained around the Ukai River, southeast of Potential Area 3, Central Sumatra Basin. The results showed that at the location, the API gravity of oil seepage was 11.7°, and was categorized as heavy oil. The gas chromatographic analysis showed that the oil was biodegraded. Using the general estimate system method, including general estimates system, GES (Pitcher *et al.*, 1989), and polyethylene glycol deposition, PEG (Hiraishi *et al.*, 1995), the bacteria types at seepage sites based on their molecular isolation were Burkholderia multivorans ATCC BAA-247 and Moraxella species osloensis strain NCTC 10465.

These bacteria were able to live and degrade oil at 500-600 m depth (Hadimuljono & Firdaus, 2021). This was confirmed by heavy oil production in Area 0 at Duri Field with depths of 120 – 350 m-ss, Rantau Bais having 190 – 300 m-ss, and Kulin with 285 – 400 m-ss. Furthermore, these oil fields have an API gravity range of around 15 – 22.7°API (Winderasta *et al.*, 2018). The heavy oil analysis in Area 0 was also proven in Batang-2 Well (151.8 – 155.4 m-ss), Duri-1 Well (140.2 – 169.5 m-ss), Kulin-1a Well (287.2 – 396.2 m-ss), and Rantaubais-2 Well (206.3 – 296.9 m-ss) with respective API gravities of 22°, 22.7°, 19°, and 22°.

Efforts to verify heavy oil in the potential areas were expressed in the evaluation of well log data shown in **Figure 1** denoted with red dot points, which spread over Area 0, Potential Areas 1-4, and Potential Areas 6. As for Potential Areas 5 and 7, no data were obtained hence well log was not analyzed. The results showed that these potential areas have heavy oil. Similarly, the detailed analysis of well logs in the shallow zone at Well BTG-2 (Area 0), Well PDL-1, and Well WLS-01 in Area 4 with data on gamma rays, SP, resistivity, neutron-density (ND), and acoustic logs indicated heavy oil's presence.

According to **Figure 7,** when the gamma-ray and resistivity log data were combined,

shallow hydrocarbon zones were observed in the BTG-2 Wells (gross interval 165 - 400 m-ss), PDL-1 (283.5 - 343 m-ss), and WLS-1 (342 - 410 m-ss). The quantitative analysis of all well log data showed that the porosity in these wells was quite high, which is > 25%, while water saturation was low at < 30%, and the reservoir zone was quite thick, indicating a good ability to store oil. Information on supporting parameters, such as formation water resistivity and rock electrical parameters was obtained from the literature and it was observed that the two features characterizing shallow hydrocarbon-bearing rock formations include relatively fresh formation water and high porosity sandstones (Asquith and Krygowski, 2004).

The test results (DST #2) for the BTG-2 Well produced 19 BOPD and 13 barrels of water per day (BWPD), while the PDL-1 Well results reveal that the porous hydrocarbon bearing zone in the well flows from one to two BOPD and 30 BWPD. The laboratory oil characterization test for oil samples showed specific gravity values of 22ºAPI for the BTG-2 and 18ºAPI for the PDL-1 Wells. Furthermore, the DST results for the WLS-1 Well, obtained in the form of thick, very slow lump flow without clear water cutting were recorded and it indicated the presence of tar material. Based on the information, tar or heavy oils, such as asphalt typically have an API value of less than 10º (Awadh & Almimar, 2015).
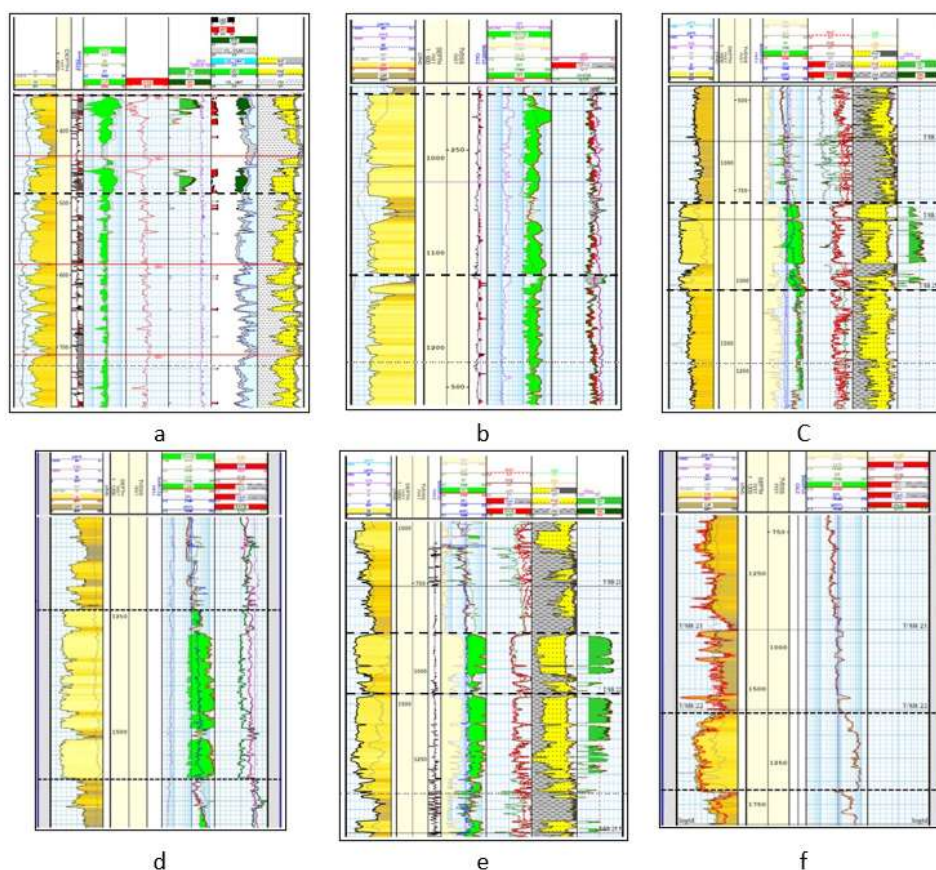

Figure 7. Qualitative well log interpretation indicates shallow hydrocarbon bearing (between dashed lines). (a) BTG-2 well at 165-400 m-ss confirmed the presence of HO based on the drill stem test (DST). (b) PDL-1 well at 283.5-343 m-ss confirmed the presence of HO based on DST; (c) WLS-1 well at 342-410 m-ss confirmed the presence of HO based on the combination of DST and mud log data. (d) BKL-1 well at 377-487.7 indicated the presence of HO, but there was no DST test. (e) LKT-1 well at 396.2-449.6 m-ss indicated the presence of HO, but there was no test yet, and (f) BCG-1 well at 459.3-524.3 m-ss indicated the presence of HO, but there was no tested yet.

Well log analysis was also performed on suspended wells, namely BKL-1, LKT-1, and BCG-1 at Potential Area 4 shown in **Figure 7**. It was observed that there are oil bearings in these wells with depths of 377 – 487.7, 396.2 – 449.6, and 459.3 – 524.3 m-ss, respectively. The problem is that there is no test/fluid sampling in these wells to confirm the identified porous zone content. However, this evidence served as support for verification of the heavy oil spots identified through surface and subsurface lineaments analyses. A similar analysis was conducted on 48 well logs in Potential Areas 1 – 3 and 6. The results generally indicate heavy oil reservoir's presence in the subsurface at 25 m - 611 m depth, which is divided into 3 categories, namely 1) proven, including Area 0, Potential Area 1 and 4, 2) probable, comprising of Potential Area 3, and 3) possible, consisting of Potential Area 2, 5, 6, 7. The 'proven category' has a high certainty of containing heavy oil due to data support from well log analysis, well and laboratory sample tests, as well as proof of production. Also, the 'probable category' has a moderate certainty level based on available data. This is because the existing data do not directly confirm the heavy oil's presence but was reflected by the well log data pattern as in the proven category. The 'possible category' indicated a heavy oil's presence based on the qualitative and quantitative interpretation results of the well log, reflecting the heavy oil window's presence with no information to counter it. Heavy oil formation in the CSB occurs at the highland's edges, where the reservoir was uplifted at a depth below 2 km. This condition causes cracks to occur, thereby resulting in increased rock permeability, which supports microbial life. This situation was evident in underground reservoirs in North Africa and the Atlantic Margin (John *et al.*, 2017).

Hydrocarbon formation in the CSB occurred at the Eocene – Oligocene age, which was an extension phase, with half grabens' formation in the N-S and NW-SE directions, followed by a rapid subsidence process. In this phase, the Pematang Group deposited consists of lacustrine – fluvio deltaic, which were considered the main source rock. Furthermore, in the Early – Middle Miocene age, there was sea flooding followed by uplift and weak folding, as well as a horizontal fault where the Sihapas Group and the Petani Formation were deposited.

The Sihapas Group lithology served as a hydrocarbon reservoir with Petani Formation being the cap rock. It is important to note that hydrocarbons in Paleogene deposits were observed to have matured at the Middle Miocene and migrated to the Neogene formations above. Tectonic processes occurred in the Plio-Pleistocene, thereby resulting in continuous uplift and folding. In this phase, Mina's Formation and Alluvial Deposits are dropped. The N-S and NW-SE trending structural patterns were reactivated, resulting in an uplift. This is proven by the existence of a thrust fold structure in the Duri field which experienced an uplift. In addition, the reservoir zone at the Bekasap and Duri formations levels was uplifted to relatively shallow depths of < 600 m (Doust & Noble, 2008; Heidrick & Aulia, 1993; Robinson & Kamal, 1988; Schenk *et al.*, 2015; Williams *et al.*, 1985). This condition is expected to allow the water washing process, biodegradation, and evaporation of the oil, as well as heavy oil formation.

It was observed that heavy oil exploitation requires hot steam injection as a method for oil recovery. However, the impact often causes environmental problems, which means it has to be replaced by electrical heating to transfer the heat into the reservoir using an electric current (Hasibuan *et al.*, 2020). This is the reason Felix & Din (2022) recommended transformer usage, which is capable of increasing and decreasing the voltage to stabilize high-voltage electrical systems. According to Martínez-Palou *et al.* (2011), transporting heavy oil from the wellhead to the refinery is quite challenging due to high viscosity, asphalt and paraffin

deposition, water content formation, salt content, and corrosion problems. Therefore, corrosion prediction is very important in calculating pipe life and equipment systems during the operation stage (Asmara & Kurniawan, 2018).

5. CONCLUSION

The multispectral merged satellite Landsat 8 OLI imagery interpreted manually and automatically with DEM SRTM and supported by regional geology understanding has successfully identified faults and join structures that developed on the earth's surface in the CSB. Manual interpretation of free air anomaly (FAA) gravity maps was able to identify the regional distribution of low and high areas, as well as lineaments that developed in the CSB.

This information provides petroleum exploration activities with an overview of the source rock location and reservoir potential. Also, the overlaying analysis between the subsurface and surface structural maps demonstrated the potential to continuously study subsurface and surface structures. Traditionally, these features' presence in subsurface structure is considered a means for petroleum migration from source rocks to reservoirs/traps. Meanwhile, from another perspective, it is likely to increase the opportunity for surface water to come in contact with oil in the reservoir, thereby facilitating the transformation of lighter oils into heavy oil.

Combined analyses of Landsat 8 operational land images (OLI), shuttle radar topographic mapping (SRTM), and free air anomaly (FAA) gravity data, verified against existing well log and fluid sampling/laboratory data, showed that both surface and subsurface lineaments approaches worked properly to identify heavy oil potential locations. Consequently, this study showed that heavy oil in the CSB is estimated to be present in existing fields, such as Duri, Batang, Kulin, and Rantaubais,

and also found potentially at dozens more spots.

The potential for heavy oil presence was estimated to be distributed at highlands' edges, particularly those facing the graben. The analytical results showed that there are about seven (7) potential areas estimated to contain heavy oil. Several well test/fluid sampling results also showed that some of these suspected spots were indeed proven to contain heavy oil. This indicates that further exploration needs to be conducted to prove heavy oil's presence at different spots in the CSB. Also, the application of this combined surface-subsurface lineament approach has to be encouraged in other sedimentary basins.

6. ACKNOWLEDGMENT

7. FUNDING

Research Programme at the Faculty of Earth Sciences and Technology, Bandung Institute of Technology, Bandung-Republic of Indonesia.

8. AUTHORS' NOTE

The authors declare that there is no conflict of interest regarding the publication of this article. The authors confirmed that the paper was free of plagiarism.

9. REFERENCES

Abd Al-Aali, H. M., Soltan, B. H., Al Mohsen, M. J., and Handhal, A. M. (2022). Identification of tar mat in zubair formation of the x oilfield, Southern Iraq. *Iraqi Geological Journal*, *55*(1), 158–166.

Agustin, F., Abdullah, C., Adiputra, R., and Sulastri, A. (2019). Analysis earthquake of suliti and siulak segments based on fullbore formation microresistivity Central Sumatra Basin. *Pacific Conference on Earthquake Engineering, 2019,*1-15.

Ahmadi, H., and Pekkan, E. (2021). Fault-based geological lineaments extraction using remote sensing and gis-a review. *Geosciences (Switzerland)*, *11*, 183–214.

Asmara, Y. P., and Kurniawan, T. (2018). Corrosion prediction for corrosion rate of carbon steel in oil and gas environment: A review. *Indonesian Journal of Science and Technology*, *3*(1), 64–74.

Asquith, G., and Krygowski, D. (2004). Chapter 1: Basic Relationships of Well Log Interpretation. *AAPG Methods in Exploration, 16*, 1-20.

Awadh, S., and Almimar, H. (2015). Statistical analysis of the relations between api, specific gravity and sulfur content in the universal crude oil. *International Journal of Science and Research*, *4*(5), 1279–1284.

Aydogan, D. (2011). Extraction of lineaments from gravity anomaly maps using the gradient calculation: Application to Central Anatolia. *Earth, Planets and Space*, *63*(8), 903–913.

Boucher, R. K. (1995). The relevance of lineament tectonics to hydrocarbon occurences in the cooper and eromanga basins, South Australia. *Petroleum Exploration Society of Australia (PESA) Journal*, *23*, 69–75.

Briggs, P. J., Baron, P. R., Fulleylove, R. J., and Wright, M. S. (1988). Development of Heavy-oil reservoirs. *Journal of Petroleum Technology*, *40*(02), 206–214.

Chakraborty, S., Panchakarla, A., Deshpande, C., Malik, S., Singh Majithia, P., Chaudhary, S., and Murthy, A. V. R. (2018). An integrated approach to characterize heavy oil in complex clastics-a case study from southern part of India. *SPE International Heavy Oil Conference and Exhibition*, *2018,*1-14.

Chen, P., Chen, P., Guo, S., and Chen, M. (2015). Optimized log evaluation method of unconsolidated sandstone heavy oil reservoirs. *International Journal of Science*, *2*(12), 109–115.

Chen, S., Zhao, Y., Zhao, L., Liu, Y., and Zhou, C. (2017). Hydrocarbon micro-seepage detection by altered minerals mapping from airborne hyper-spectral data in xifeng oilfield, China. *Journal of Earth Science*, *28*(4), 656–665.

Darling, T. (2005). *Well logging and Formation Evaluation*. United States:Elsevier.

Darmawan, D., Daud, Y., and Iskandar, C. (2021). Identification of geological structure based on gravity and remote sensing data in "X" geothermal field. *AIP Conference Proceedings*, *2320*(1), 40004.

Davy, B., Stagpoole, V., Barker, D., and Yu, J. (2012). Subsurface structure of the Canterbury region interpreted from gravity and aeromagnetic data. *New Zealand Journal of Geology and Geophysics*, *55*(3), 185–191.

Doust, H. (2017). Petroleum systems in Southeast Asian Tertiary basins. *Bulletin of the Geological Society of Malaysia*, *64*, 1–16.

Doust, H., and Noble, R. A. (2008). Petroleum systems of Indonesia. *Marine and Petroleum Geology*, *25*(2), 103–129.

Ebulue, M. M. (2022). Molecular evaluation of soil respiration in crude oil pollution. *ASEAN Journal of Science and Engineering*, *3*(2), 101–108.

Ekinci, Y. L., and Yiğitbaş, E. (2015). Interpretation of gravity anomalies to delineate some structural features of Biga and Gelibolu peninsulas, and their surroundings (north-west Turkey). *Geodinamica Acta*, *27*(4), 300–319.

Enoh, M., and Okeke, F. (2021). Automatic lineaments mapping and extraction in relationship to natural hydrocarbon in Ugwueme, South-Eastern Nigeria. *Geodesy and Cartography*, *47*(1), 34–44.

Epuh, E. E., Okolie, C. J., Daramola, O. E., Ogunlade, F. S., Oyatayo, F. J., Akinnusi, S. A., and Emmanuel, E.-O. I. (2020). An integrated lineament extraction from satellite imagery and gravity anomaly maps for groundwater exploration in the Gongola Basin. *Remote Sensing Applications: Society and Environment*, *20*, 100346.

Felix, S. A. A., and Din, M. F. M. (2022). Effect of proper treatment on mineral oils. *ASEAN Journal of Science and Engineering*, *3*(3), 281–288.

Gao, D., and Milliken, J. (2012). Cross-regional intraslope lineaments on the lower congo basin slope, offshore Angola (West Africa): Implications for tectonics and petroleum systems at passive continental margins. *AAPG Memoir*, *100*, 229–248.

Gonçalves, R., Loh, W., and Trevisan, O. (2014). An overview of heavy oil properties and its recovery and transportation methods. *Brazilian Journal of Chemical Engineering*, *31*, 571–590.

Gregor, V. A. (1997). Mannville linears in the lloydminster heavy oil area and their relationship to fractures and fluid flow in the Western Canada Sedimentary Basin. *AAPG Memoir*, *18*, 428–474.

Gunningham, N. (2013). Managing the energy trilemma: The case of Indonesia. *Energy Policy*, *54*, 184–193.

Guo, G., and George, S. A. (1999). An analysis of surface and subsurface lineaments and fractures for oil and gas exploration in the mid-continent region, *USDOE Office of Fossil Energy (FE) (US)*, *5611*, 1-36.

Guo, G., George, S. A., and Lindsey, R. P. (1997). Analysis of surface lineaments and fractures for hydrocarbon exploration and production optimization in the mid-continent region. *SPE Annual Technical Conference and Exhibition*, SPE-38714-MS, 1-15.

Guo, K., Li, H., and Yu, Z. (2016). In-situ heavy and extra-heavy oil recovery: A review. *Fuel*, *185*, 886–902.

Hadimuljono, J. S., and Firdaus, N. (2021). Determination of biodegradation zone in Central Sumatra Basin. *Scientific Contributions Oil and Gas*, *44*(1), 55–63.

Hasibuan, M. Y., Regina, S., Wahyu, R., Situmorang, D., Azmi, F., Syahputra, R., Batubara, L. P. Y., Prabowo, F., Setiawan, A., and Afin, M. F. (2020). Electrical heating for heavy oil: Past, current, and future prospect, *Preprints*, *1*, 1-18.

Head, I. M., Jones, D. M., and Larter, S. R. (2003). Biological activity in the deep subsurface and the origin of heavy oil. *Nature*, *426*(6964), 344–352.

Heidrick, T., and Aulia, K. (1993). A structural and tectonic model of the coastal plains block, Central Sumatra Basin, Indonesia. *22nd Annual Convention Proceedings*, *1*, 285–315.

Hein, F. J. (2006). Heavy oil and oil (tar) sands in North America: An overview and summary of contributions. *Natural Resources Research*, *15*(2), 67–84.

Hein, F. J. (2017). Geology of bitumen and heavy oil: An overview. *Journal of Petroleum Science and Engineering*, *154*, 551–563.

Hildenbrand, T. G., Stuart, W. D., and Talwani, P. (2001). Geologic structures related to New Madrid earthquakes near Memphis, Tennessee, based on gravity and magnetic interpretations. *Engineering Geology*, *62*(1), 105–121.

Hiraishi, A., Kamagata, Y., and Nakamura, K. (1995). Polymerase chain reaction amplification and restriction fragment length polymorphism analysis of 16S rRNA genes from methanogens. *Journal of Fermentation and Bioengineering*, *79*(6), 523–529.

Hwang, R. J., Heidrick, T., Mertani, B., Qivayanti, and Li, M. (2002). Correlation and migration studies of North Central Sumatra oils. *Organic Geochemistry*, *33*(12), 1361–1379.

John, P., Mas'ud, B., Stephen, B., and David, M. (2017). Subsurface biodegradation of crude oil in a fractured basement reservoir, Shropshire, UK. *Journal of the Geological Society*, *174*(4), 655–666.

Leythaeuser, D. (2005). Origin, migration and accumulation of petroleum. *Encyclopedia of Hydrocarbons*, *2005*, 65–84.

Li, Y., Chen, S., Liu, X., Wu, B., Zhang, J., He, X., Mou, F., and Luo, L. (2022). Study on the logging response characteristics and the quantitative identification method of solid bitumen at different thermal evolution stages. *Fuel*, *316*, 123424.

Macellari, C. E. (2021). Recent uplift and the origin of hydrodynamic traps in the Llanos Basin of Colombia. *Marine and Petroleum Geology*, *132*, 105198.

Markovic, S., Bryan, J. L., Turakhanov, A., Cheremisin, A., Mehta, S. A., and Kantzas, A. (2020). In-situ heavy oil viscosity prediction at high temperatures using low-field NMR relaxometry and nonlinear least squares. *Fuel*, *260*, 116328.

Martínez-Palou, R., Mosqueira, M., Zapata-Rendón, B., Mar, E., Bernal-Huicochea, C., Clavel-Lopez, J., and Aburto, J. (2011). Transportation of heavy and extra-heavy crude oil by pipeline: A review. *Journal of Petroleum Science and Engineering - J PET SCI ENGINEERING*, *75*, 274–282.

Mertosono, S., and Nayoan, G. A. S. (1974). The tertiary basinal area of Central Sumatra. *Indonesian Petroleum Association Proceeding*, *1974*, 67–76.

Meyer, R. F., and Attanasi, E. D. (2003). Heavy oil and natural bitumen-strategic petroleum resources. *World*, *434*, 650-700.

Meyer, R. F., Attanasi, E. D., and Freeman, P. A. (2007). Heavy oil and natural bitumen resources in geological basins of the world: Map showing klemme basin classification of sedimentary provinces reporting heavy oil or natural bitumen. *US Geol. Surv. Open-File Rep*, *2007*, 1084.

Naik, V., Mudhfar, D., Pal, A., Karam, E. M., Attar, I., and M. Al-Haddad, S. (2018). An innovative approach to test heavy oil in burgan reservoir of greater burgan field. *SPE International Heavy Oil Conference and Exhibition, SPE-193793-MS*, 1-10.

Ombati, D., John, G., k'Orowe, M., and Nyakundi, E. (2022). Delineation of subsurface structures using gravity data of the shallow offshore, Lamu Basin, Kenya. *International Journal of Geophysics*, *2022*, 1–12.

Pallone, S. (2009). Indonesia's oil crisis: How Indonesia became a net oil importer. *The Journal of International Policy Solutions*, *10*(3), 1–10.

Parnell, J., Baba, M., Bowden, S., Muirhead, D., John, P., Mas'ud, B., Stephen, B., and David, M. (2017). Subsurface biodegradation of crude oil in a fractured basement reservoir, Shropshire, UK. *Journal of the Geological Society*, *174*(4), 655–666.

Penner, L. A., and Mollard, J. D. (1991). Correlated photolineament and geoscience data on eight petroleum and potash study projects in southern saskatchewan. *Canadian Journal of Remote Sensing*, *17*(2), 174–184.

Petrovic, A., Khan, S. D., and Chafetz, H. S. (2008). Remote detection and geochemical studies for finding hydrocarbon-induced alterations in Lisbon valley, Utah. *Marine and Petroleum Geology*, *25*(8), 696–705.

Pitcher, D. G., Saunders, N. A., and Owen, R. J. (1989). Rapid extraction of bacterial genomic DNA with guanidium thiocyanate. *Letters in Applied Microbiology*, *8*(4), 151–156.

Rahayu, Y. S., Yuliani, and Trimulyono, G. (2019). Isolation and identification of hydrocarbon degradation bacteria and phosphate solubilizing bacteria in oil contaminated soil in Bojonegoro, East Java, Indonesia. *Indonesian Journal of Science and Technology*, *4*(1), 134–147.

Robinson, K. M., and Kamal, A. (1988). Hydrocarbon generation, migration and entrapment in the Kampar Block, Central Sumatra. *17th Annual Convention Proceedings*, 211–256.

Rodriguez, N. D., and Paul Philp, R. (2012). Productivity and paleoclimatic controls on source rock character in the Aman Trough, north central Sumatra, Indonesia. *Organic Geochemistry*, *45*, 18–28.

Rodriguez, N., and Philip, R. (2015). Source rock facies distribution predicted from oil geochemistry in the Central Sumatra Basin, Indonesia. *AAPG Bulletin*, *99*, 2005–2022.

Sandwell, D., Müller, D., Smith, W., Garcia, E., and Francis, R. (2014). New global marine gravity from CryoSat-2 and Jason-1 reveals buried tectonic structure. *Science*, *346*, 65–67.

Satyakumar, A. V, Pandey, A. K., Singh, A. P., and Tiwari, V. M. (2022). Delineation of structural and tectonic features in the Mahanadi basin, eastern India: New insights from remote sensing and land gravity data. *Journal of Asian Earth Sciences*, *227*, 105116.

Schenk, C. J., Charpentier, R. R., Klett, T. R., Tennyson, M. E., Mercier, T. J., Brownfield, M. E., Pitman, J. K., Gaswirth, S. B., and Leathers-Miller, H. M. (2015). Assessment of shale-oil resources of the Central Sumatra Basin, Indonesia. *Fact Sheet*, *2015*, 1-2.

Schumacher, D. (1996). Hydrocarbon-induced alteration of soils and sediments. *AAPG Memoir the American Association of Petroleum Geologists*, *66*, 71–89.

Setiadi, I., Widodo, J., and Nainggolan, T. B. (2021). Geological interpretation of offshore Central Sumatra basin using topex satellite gravity data. *IOP Conference Series: Earth and Environmental Science*, *944*(1), 12034.

Susantoro, T. M., Saepuloh, A., Agustin, F., Wikantika, K., and Harsolumakso, A. H. (2020). Clay mineral alteration in oil and gas fields: integrated analyses of surface expression, soil spectra, and X-ray diffraction data. *Canadian Journal of Remote Sensing*, *46*(2), 237–251.

Susantoro, T. M., Wikantika, K., Puspitasari, A. S. S., and Saepuloh, A. (2017). Impact of oil and gas field in sugar cane condition using landsat 8 in Indramayu area and its surrounding, West Java province, Republic of Indonesia. *IOP Conference Series: Earth and Environmental Science*, *54*(012019), 12019.

Sutadiwiria, G., and Azwar, N. (2011). The effect of unplanned shutdown to world's largest steamflood project, duri field Indonesia. *SPE Heavy Oil Conference and Exhibition*, SPE-150516-MS, 1-7.

Suwarna, N., Budhtrisna, T., Santosa, S., and Andi Mangga, S. (1994). Geological Map of the Rengat Quadrangle, Sumatera, scale 1: 250.000. *Geological Research and Development Centre, Bandung*.

Widarsono, B., Setiawan, H. L., Susantoro, T. M., Suliantara, S., Hadimuljono, J. S., Yensusminar, D., Julikah, J., and Prayoga, O. A. (2021). An integrated approach for revisiting basin-scale heavy oil potential of the Central Sumatra Basin. *Scientific Contributions Oil and Gas*, *44*(1), 01–20.

Williams, H. H., and Eubank, R. T. (1995). Hydrocarbon habitat in the rift graben of the Central Sumatra Basin, Indonesia. *Geological Society Special Publication*, *80*(80), 331–371.

Williams, H. H., P. A. Kelley, J. S. Janks, and R. M. Christensen. (1985). The Paleogene rift basin source rocks of Central Sumatra. *14th Annual Convention Proceedings*, *2*, 57-90.

Winderasta, W., Evi, S., Budiman, A., and Amlan, M. (2018). Managing reservoir surveillance in duri steam flood field. *Proceedings, Indonesian Petroleum Association*, *42*, 1-10.

Zhou, Z., Lu, J., Wu, H., and Yang, L. (2021). NMR response of maturity parameters and biodegradation grade of heavy oil. *Petroleum Science and Technology*, *39*(11–12), 441–449.